

Coherent excitation energy transfer in a photosynthetic heat engine: Effects of non-Markovian quantum environment

Jie Fang,* Zi-Hao Chen,* Yu Su, Zi-Fan Zhu, Yao Wang,[†] Rui-Xue Xu,[‡] and YiJing Yan
Department of Chemical Physics, University of Science and Technology of China, Hefei, Anhui 230026, China

Excitation energy transfer (EET) and electron transfer (ET) are crucially involved in photosynthetic processes. In reality, the photosynthetic reaction center constitutes an open quantum system of EET and ET, which manifests an interplay of pigments, solar light and phonon baths. In this work, this open system is investigated by using a mixed dynamic approach. The influence of phonon bath is treated via the exact dissipaton equation of motion while that of photon bath is via Lindblad master equation. Effects of non-Markovian quantum phonon bath on the coherent transfer dynamics and its manipulations on the current–voltage behaviors associated mainly with steady states are specifically explored.

I. INTRODUCTION

Photosynthesis is one of the most important processes in biological systems, by which plants and other organisms convert sunlight energy into chemical energy. It is found that excitation energy transfer (EET) and electron transfer (ET) are crucially involved in the photosynthetic process. To be concrete, sunlight is absorbed to create an excited state, followed by EET among pigments to reaction center, where ET happens resulting in charge separation converting excitation energy to chemical energy.

In recent years, the role of quantum coherence in the EET and ET processes of photosynthesis has got great interest.^{1–9} The core complex is the main participant in the EET and ET processes of reaction center. In reality, it constitutes an open quantum system, which manifests an interplay between pigments, solar light and phonon baths. The involved dynamics could be non-Markovian in case that the coupling strength between pigments and the phonon environment be comparable to that between pigments themselves, as well as the timescale of EET/ET around that of the phonon bath memory.

Unlike the light-harvesting systems, which have been theoretically intensively studied,^{10–19} dynamics of the EET/ET processes in the reaction center is relatively rarely explored. So far theoretical studies on EET/ET in the photosynthetic reaction center are mainly based on some approximate methods, such as the Redfield equation,^{4,20} polaron master equation,²¹ and Pauli master equation.²² The quantum coherence enhanced effect on electric current was once exhibited in Ref. 23. However, Creatore and co-workers pointed out that the master equation used in Ref. 23 were unstable and the numerical evolutions there did not retain the positivity of density matrix, resulting in artificial behaviors which would diverge with time going on, see the details in Supplemental Material of Ref. 22. Hence accurate simulations are needed, together with assessments on approximate approaches.

In this work, we study this open system problem using a mixed dynamic approach. The photon bath (light) influence is treated adopting the Lindblad equation,^{24,25} while that of the phonon environment is via the dissipaton equation of motion (DEOM) method.^{26,27} The

DEOM is a non-Markovian and nonperturbative approach, constructed on basis of a quasi-particle, dissipaton representation for hybridized collective bath dynamics. For reduced system dynamics, the DEOM is equivalent to the hierarchical equation of motion (HEOM) formalism,²⁸ which is established via time derivative on the influence functional path integral or stochastic fields methods.^{29–33} Both HEOM and DEOM are exact under Gaussian bath statistics. The DEOM is more convenient and straightforward to study environmental dynamics related problems, such as polarizations under external fields.^{15,27,34}

In this work, the phonon bath will also be treated via the semigroup Lindblad master equation for comparison with DEOM. Meanwhile the quantum coherence versus non-Markovianity of phonon bath will be demonstrated. Effect of the quantum statistical nature of phonon bath is also explored. The remainder of paper is organized as follows. In Sec. II A, we introduce a five-level model^{6,21–23} applied in our study, which captures the main features of the EET and ET processes in the photosynthetic reaction center heat engine. The associated Hamiltonian and bath functions are then described. The mixed DEOM–Lindblad dynamic equations are presented in Sec. II B. The construction of Lindblad master equation is briefly outlined in Appendix. Numerical simulations on transfer dynamics and current–voltage behaviors are demonstrated and discussed in Sec. III. The paper is summarize in Sec. IV.

II. THEORETICAL DESCRIPTION

In this section, we begin with the setup of total system–plus–baths composite exploited in this study, where the system is described by a five-level model.^{6,21–23} This five-level model system, based on the photosystem II core complex, not only characterizes the main features of EET and ET processes, but also takes into account the important interactions involved. The system Hamiltonian and bath coupling statistics as well as the adopted mixed dynamic approach are given after that. For brevity, we set $\hbar = 1$ and $\beta = 1/(k_B T)$ throughout the paper, with k_B being the Boltzmann constant and T the temperature.

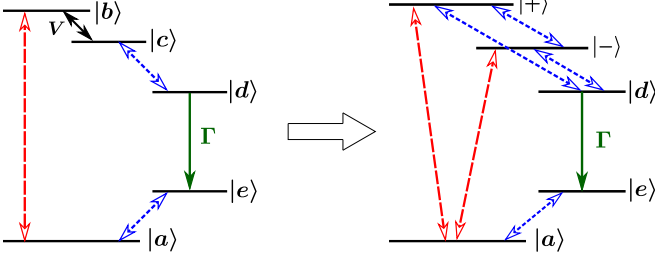
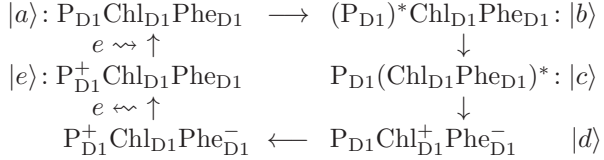


FIG. 1: Sketch of the total composite model before and after the diagonalization of system Hamiltonian.

A. Five-site model of system and bath statistics

Let us first introduce the system from the biological perspective.⁶ The photosystem II reaction center core complex contains four chlorophylls (special pair P_{D1} and P_{D2} and accessory chlorophylls Chl_{D1} and Chl_{D2}) and two pheophytins (Phe_{D1} and Phe_{D2}), arranged into two branches (D1 and D2). Only the D1 branch plays an active role in the photo-induced electron transfer:



The D1 branch, P_{D1}Chl_{D1}Phe_{D1}, is firstly excited from |a> to |b> via the absorption of photons. From |b> to |c> is the EET, followed by the charge separation resulting in state |d> where the positive and negative charges are rapidly spatially separated. For simplicity, a charge-separated state |d> is coarsely used to represent both states. From |d> to |e>, an electron is released from the system to perform work. At last, the system captures an electron from the surroundings to complete the cycle and returns to the ground state |a>.

According to the above description, the system Hamiltonian can be written as

$$H_s = \sum_{m \in I} E_m |m\rangle\langle m| + V(|b\rangle\langle c| + |c\rangle\langle b|), \quad (1)$$

with $I \equiv \{a, b, c, d, e\}$. To phenomenologically describe the electron release from |d> to |e>, a superoperator can be introduced as

$$L_\Gamma \hat{O} = -\frac{\Gamma}{2} [\hat{O}|d\rangle\langle d| + |d\rangle\langle d|\hat{O} - 2|e\rangle\langle d|\hat{O}|d\rangle\langle e|]. \quad (2)$$

Here, Γ is the rate of release.

For the system-plus-baths composite, the total Hamiltonian reads

$$H_T = H_s + H_{SB}^{(I)} + H_{SB}^{(II)} + h_B^{(I)} + h_B^{(II)} \quad (3)$$

Here, the system Hamiltonian is as in Eq. (1), while the bath Hamiltonians are

$$h_B^{(I)} = \sum_k \varepsilon_k b_k^\dagger b_k \quad \text{and} \quad h_B^{(II)} = \sum_j \omega_j a_j^\dagger a_j \quad (4)$$

for the photon bath and phonon bath, respectively. The system-bath interaction Hamiltonians read

$$H_{SB}^{(I)} = \hat{Q}_1^{(I)} \hat{F}_1^{(I)}, \quad (5a)$$

$$H_{SB}^{(II)} = \sum_{\mu=2}^5 \hat{Q}_\mu^{(II)} \hat{F}_\mu^{(II)}, \quad (5b)$$

with $\hat{Q}_1^{(I)} = |a\rangle\langle b| + |b\rangle\langle a|$, $\hat{Q}_2^{(II)} = |c\rangle\langle d| + |d\rangle\langle c|$, $\hat{Q}_3^{(II)} = |e\rangle\langle a| + |a\rangle\langle e|$, $\hat{Q}_4^{(II)} = |b\rangle\langle b|$, and $\hat{Q}_5^{(II)} = |c\rangle\langle c|$, whereas $\hat{F}_1^{(I)} = \frac{1}{\sqrt{2}} \sum_k \tilde{c}_k (b_k + b_k^\dagger)$ and $\hat{F}_{\mu=2 \sim 5}^{(II)} = \frac{1}{\sqrt{2}} \sum_j c_{\mu j} (a_j + a_j^\dagger)$. These settings are depicted in the left panel of Fig. 1 and constitute Gaussian bath couplings. Their influences on the system can be completely characterized by the spectral densities,

$$J_1^{(I)}(\omega > 0) = \frac{\pi}{2} \sum_k \tilde{c}_k^2 \delta(\omega - \varepsilon_k), \quad (6a)$$

and (for $\mu, \nu = 2 \sim 5$)

$$J_{\mu\nu}^{(II)}(\omega > 0) = \frac{\pi}{2} \sum_j c_{\mu j} c_{\nu j} \delta(\omega - \omega_j). \quad (6b)$$

In Fig. 1, red and blue dash arrows represent the state transfers induced by photon and phonon baths, respectively. The system Hamiltonian eigenstates are |a>, |d>, |e> and

$$\begin{bmatrix} |+\rangle \\ |-\rangle \end{bmatrix} = \mathbf{U} \begin{bmatrix} |b\rangle \\ |c\rangle \end{bmatrix} \equiv \begin{bmatrix} u_{11} & u_{12} \\ u_{21} & u_{22} \end{bmatrix} \begin{bmatrix} |b\rangle \\ |c\rangle \end{bmatrix} \quad (7)$$

with \mathbf{U} being the real and orthogonal transformation matrix which diagonalizes H_s . Inversely

$$\begin{bmatrix} |b\rangle \\ |c\rangle \end{bmatrix} = \begin{bmatrix} u_{11} & u_{21} \\ u_{12} & u_{22} \end{bmatrix} \begin{bmatrix} |+\rangle \\ |-\rangle \end{bmatrix}. \quad (8)$$

Correspondingly, we can recast

$$\begin{aligned}
 \hat{Q}_1^{(I)} &= u_{11} (|a\rangle\langle +| + |+\rangle\langle a|) + u_{21} (|a\rangle\langle -| + |-\rangle\langle a|), \\
 \hat{Q}_2^{(II)} &= u_{12} (|+\rangle\langle d| + |d\rangle\langle +|) + u_{22} (|-\rangle\langle d| + |d\rangle\langle -|), \\
 \hat{Q}_4^{(II)} &= u_{11}^2 |+\rangle\langle +| + u_{21}^2 |-\rangle\langle -| + u_{11} u_{21} (|+\rangle\langle -| + |-\rangle\langle +|), \\
 \hat{Q}_5^{(II)} &= u_{12}^2 |+\rangle\langle +| + u_{22}^2 |-\rangle\langle -| + u_{12} u_{22} (|+\rangle\langle -| + |-\rangle\langle +|),
 \end{aligned}$$

and $\hat{Q}_3^{(II)}$ is not affected. The transformed interaction patterns are exhibited in the right panel of Fig. 1.

B. Mixed DEOM–Lindblad dynamic approach

In the total composite space, the total density operator $\rho_T(t)$ evolves as

$$\dot{\rho}_T(t) = -i[H_T, \rho_T(t)] + L_\Gamma \rho_T(t), \quad (9)$$

with H_T and L_Γ defined in Eqs. (3) and (2), respectively. In the proposed mixed dynamic approach, light is treated

as photon bath via the Lindblad master equation, detailed in Appendix. Thus an additional superoperator for the action of light is now introduced as

$$L^{(I)} = \gamma_+ u_{11}^2 L_+ + \gamma_- u_{21}^2 L_- \quad (10)$$

with $\gamma_{\pm} \equiv 2J_1^{(I)}(\omega_{\pm a})$ the dissipative rate and

$$L_{\pm} \hat{O} = (1 + \bar{n}_{\pm}) \left(\langle \pm | \hat{O} | \pm \rangle |a\rangle\langle a| - \frac{1}{2} \{ | \pm \rangle\langle \pm |, \hat{O} \} \right) + \bar{n}_{\pm} \left(\langle a | \hat{O} | a \rangle | \pm \rangle\langle \pm | - \frac{1}{2} \{ |a\rangle\langle a|, \hat{O} \} \right), \quad (11)$$

where $\bar{n}_{\pm} \equiv \bar{n}_{\pm a}$; cf. Appendix.

To explore non-Markovian and non-perturbative influence of phonon bath, we adopt the well-established DEOM approach. It starts with the exponential expansion form of bath coupling correlation functions,

$$\tilde{C}_{\mu\nu}^{(II)}(t) = \frac{1}{\pi} \int_{-\infty}^{\infty} d\omega \frac{e^{-i\omega t} J_{\mu\nu}^{(II)}(\omega)}{1 - e^{-\beta\omega}} = \sum_{\kappa} \xi_{\kappa}^{\mu\nu} e^{-\gamma_{\kappa}^{\mu\nu} t}. \quad (12)$$

The first identity is the fluctuation-dissipation theorem.^{35,36} The standard DEOM algebra gives rise to^{26,27}

$$\dot{\rho}_{\mathbf{n}}^{(n)} = - \left[i\mathcal{L}_s - L_{\Gamma} - L^{(I)} + \sum_{\mu\nu\kappa} n_{\kappa}^{\mu\nu} \gamma_{\kappa}^{\mu\nu} \right] \rho_{\mathbf{n}}^{(n)} - i \sum_{\mu\nu\kappa} \left[\mathcal{A}_{\mu} \rho_{\mathbf{n}_{\mu\nu\kappa}^+}^{(n+1)} + n_{\kappa}^{\mu\nu} \mathcal{C}_{\kappa}^{\mu\nu} \rho_{\mathbf{n}_{\mu\nu\kappa}^-}^{(n-1)} \right], \quad (13)$$

with $\mathcal{L}_s \hat{O} \equiv [H_s, \hat{O}]$ and

$$\mathcal{A}_{\mu} \hat{O} \equiv [\hat{Q}_{\mu}^{(II)}, \hat{O}], \quad (14a)$$

$$\mathcal{C}_{\kappa}^{\mu\nu} \hat{O} \equiv \xi_{\kappa}^{\mu\nu} \hat{Q}_{\nu}^{(II)} \hat{O} - (\xi_{\kappa}^{\mu\nu})^* \hat{O} \hat{Q}_{\nu}^{(II)}. \quad (14b)$$

This is the mixed DEOM–Lindblad formalism. The term of index $\bar{\kappa}$ is associated with that of κ by $\gamma_{\bar{\kappa}}^{\mu\nu} \equiv (\gamma_{\kappa}^{\mu\nu})^*$. The indices of density matrices are denoted as $\mathbf{n} = \{n_{\kappa}^{\mu\nu}\}$, an ordered set of the bosonic dissipator's occupation numbers, $n_{\kappa}^{\mu\nu} = 0, 1, \dots$, and $n = \sum_{\mu\nu\kappa} n_{\kappa}^{\mu\nu}$ the total number. $\mathbf{n}_{\mu\nu\kappa}^{\pm}$ differs from \mathbf{n} only at the specified $n_{\kappa}^{\mu\nu}$ by ± 1 . $\rho_{\mathbf{0}}^{(0)}$ is just the reduced system density operator, while the others, $\rho_{\mathbf{n}}^{(n \geq 1)}$, coupled to $\rho_{\mathbf{0}}^{(0)}$ in a hierarchical manner, are dissipator density operators.

III. NUMERICAL DEMONSTRATIONS AND DISCUSSIONS

For numerical simulations, we adopt the Drude model for the phonon bath spectral densities (for $\mu, \nu = 2 \sim 5$),

$$J_{\mu\nu}^{(II)}(\omega) = \frac{2\eta_{\mu\nu}\lambda_{\nu}\gamma_{\nu}\omega}{\omega^2 + \gamma_{\nu}^2}. \quad (15)$$

We set parameters as in Table I. They are selected in accordance with Refs. 21–23. The setup of system Hamil-

Parameters	Units	Values
E_a	cm^{-1}	0
E_b	cm^{-1}	14856
E_c	cm^{-1}	14736
E_d	cm^{-1}	13245
E_e	cm^{-1}	1611
V	cm^{-1}	30
γ_{\pm}	cm^{-1}	0.005
\bar{n}_{\pm}		60000
T	K	300
λ_2	cm^{-1}	140
γ_2	cm^{-1}	140
λ_3	cm^{-1}	200
γ_3	cm^{-1}	200
λ_4	cm^{-1}	100
γ_4	cm^{-1}	10
λ_5	cm^{-1}	100
γ_5	cm^{-1}	10

TABLE I: Parameters used in the simulations.

tonian results in the following \mathbf{U} –matrix in Eq. (7),

$$\mathbf{U} = \begin{bmatrix} 0.973 & -0.230 \\ 0.230 & 0.973 \end{bmatrix}.$$

In simulations, the $\{\eta_{\mu\nu}\}$ parameters are set as

$$\begin{bmatrix} \eta_{22} & \eta_{23} & \eta_{24} & \eta_{25} \\ \eta_{32} & \eta_{33} & \eta_{34} & \eta_{35} \\ \eta_{42} & \eta_{43} & \eta_{44} & \eta_{45} \\ \eta_{52} & \eta_{53} & \eta_{54} & \eta_{55} \end{bmatrix} = \begin{bmatrix} 1 & 0 & 0 & 0 \\ 0 & 1 & 0 & 0 \\ 0 & 0 & 1 & \eta \\ 0 & 0 & \eta & 1 \end{bmatrix}.$$

We choose $\eta = 1$ and $\eta = -1$ to represent the fully correlated and anti-correlated scenarios of the involved two fluctuating modes, $\hat{Q}_4^{(II)} = |b\rangle\langle b|$ and $\hat{Q}_5^{(II)} = |c\rangle\langle c|$, respectively. Note their real effects shall be considered with the eigenstates of system and will be varied if the sign and value of the coherent coupling V change. The Γ parameter in Eq. (2) will be varied in the following demonstration.

Figure 2 depicts the transient dynamics obtained from different approaches. The black, DEOM curves are evaluated via the mixed DEOM–Lindblad formalism proposed in Sec. II B. Both the expansion of phonon bath correlation functions and the hierarchy of dynamic equations are converged. The red curves, in the classical bath limit, are results of DEOM–Lindblad with only real parts of phonon bath correlation functions involved. Thus the quantum nature of environment can be observed via comparison between black and red curves. The blue, Lindblad results are obtained by applying the Lindblad master equation for both photon and phonon bath operations, cf. Eqs. (29)–(30) of Appendix. Therefore the non-Markovian correlated environmental effects can be highlighted in comparison between black and blue curves.

In Fig. 2, we choose cases where $\Gamma = 100$ and 500 cm^{-1} , both simulated for $\eta = -1$ and $\eta = 1$. The system is set to be at $|a\rangle$ initially. The following features can be observed from Fig. 2. (i) There are no corresponding Lindblad (blue) curves in the panels of $\text{Im}\rho_{bc}$ because its results retain zero for the present system and initial

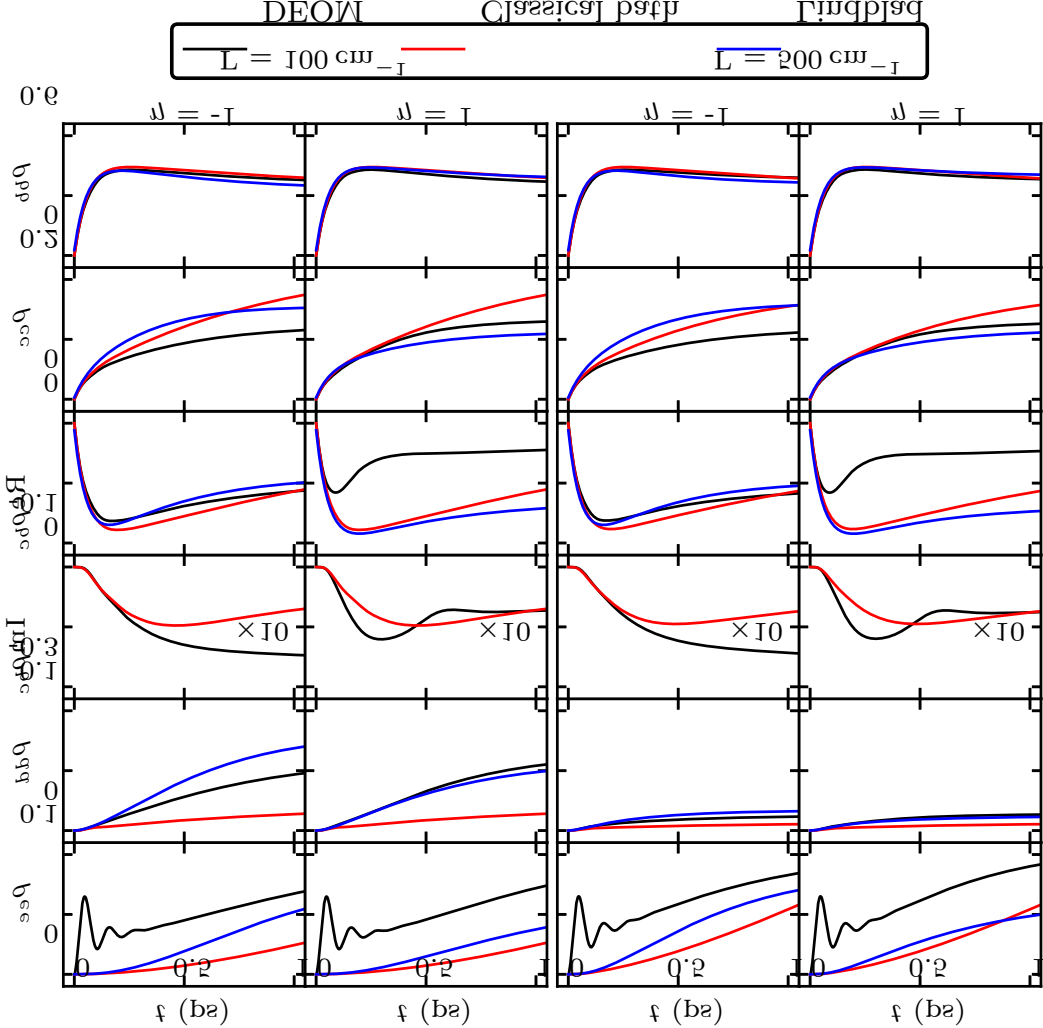


FIG. 2: Time evolutions via the mixed DEOM–Lindblad (black), DEOM–Lindblad under the classical bath limit (red), complete Lindblad (blue) methods with varied Γ and η parameters.

state. (ii) In overall panels, Lindblad (blue) results and those in the classical bath limit (red) are quite close in short time, except $\text{Im}\rho_{bc}$ due to (i). Both of them show little quantum coherent behavior. (iii) For the results by the mixed DEOM–Lindblad (black) simulation, quantum coherence is more apparently exhibited in the panels of Rep_{bc} , $\text{Im}\rho_{bc}$, and ρ_{ee} . (iv) The coherent behavior of (iii) is found independent of Γ [cf. Eq. (2)] but the anti-correlated bath fluctuations with $\eta = -1$ lead to faster dephasing processes than the correlated ones with $\eta = 1$ for the present system. (v) $\Gamma = 100$ and 500 cm^{-1} give similar transient behaviors except ρ_{dd} [cf. Eq. (2)]. Effects of Γ on steady states and the associated current–voltage properties are to be demonstrated in Fig. 3.

As in the literature,^{6,21–23} we may view the composite as a biological heat engine, with the steady-state current,

$$j = e\Gamma\rho_{s;dd}^{\text{st}} \quad (16)$$

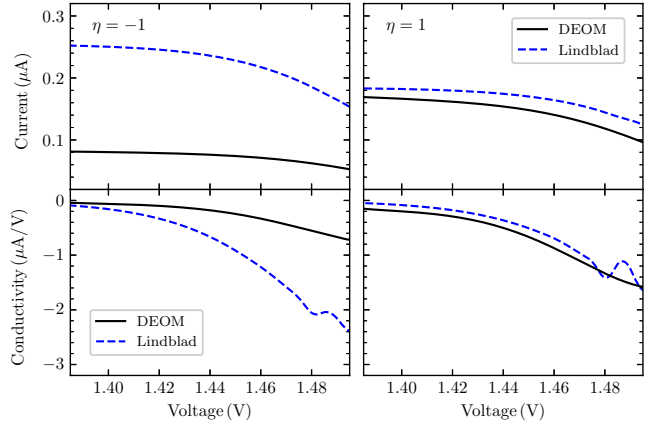


FIG. 3: Current and conductivity versus the effective voltage with the Γ parameter ranging about 900 down to 6 cm^{-1} . The black solid curves are from the mixed DEOM–Lindblad simulations while the blue dash curves are from the complete Lindblad simulations.

and the effective voltage Φ via

$$e\Phi = E_d - E_e + k_B T \ln \frac{\rho_{s;dd}^{\text{st}}}{\rho_{s;ee}^{\text{st}}}. \quad (17)$$

Here, e is the electron charge. Figure 3 depicts the current (upper-panels) and conductivity $dj/d\Phi$ (lower-panels) versus the voltage with Γ ranging about 900 down to 6 cm^{-1} . Results from the mixed DEOM–Lindblad (black-solid) and complete Lindblad (blue-dash) are shown for comparison. Note that under the classical bath limit, $\rho_{s;dd}^{\text{st}} = 0$, leading to both current and voltage undefined. Negative conductivity is observed owing to the setup of the present modeled heat engine. The Lindblad exhibits some illusive unstable behaviors. The mixed DEOM–Lindblad results demonstrate certain manipulation, switch analogue, effects by adjusting the correlation, η -parameter, between different environmental couplings.

IV. SUMMARY

In this work, we propose a mixed DEOM–Lindblad approach to study the transient dynamics and steady-state current–voltage behaviors of a modeled photosynthetic heat engine. The photon bath (light) influence is treated via the Lindblad dissipative superoperator while that of the phonon environment is via the exact DEOM method taking into account the non-Markovian and non-perturbative effects. The correlation between photon and phonon baths’ couplings on the reduced system are also included in the construction of the DEOM–Lindblad formalism. The transfer dynamics and steady-state current–voltage behaviors are demonstrated with different approaches, the mixed DEOM–Lindblad, complete Lindblad, DEOM–Lindblad with classical bath limit, for comparison. Distinguished from the other two methods, the mixed DEOM–Lindblad simulation results exhibit the transferring coherence up to a few hundreds femtoseconds and a switch–analogue environment manipulation effect on the electric current. As DEOM is an accurate method, the present observed properties are expected to be extended to more complex and realistic systems.

Acknowledgments

Support from the Ministry of Science and Technology of China (Nos. 2017YFA0204904 and 2021YFA1200103) and the National Natural Science Foundation of China (Nos. 22103073 and 22173088) is gratefully acknowledged. Y. Wang and Z. H. Chen thank also the partial support from GHfund B (20210702).

Appendix: Constructional detail of Lindblad master equation

In this appendix, we give the constructional detail of the Lindblad master equation. Consider a general form

of system–plus–bath total Hamiltonian,

$$H_{\text{T}} = H_{\text{S}} + \sum_{\mu} \hat{Q}_{\mu}^{\text{S}} \hat{F}_{\mu}^{\text{B}} + h_{\text{B}}. \quad (18)$$

The time-local quantum dissipation equation for the reduced system density operator, via cumulant partial ordering prescription with neglecting bath dispersion, is obtained as^{37,38}

$$\dot{\rho}_{\text{S}}(t) = -i\mathcal{L}_{\text{S}}\rho_{\text{S}}(t) - \sum_{\mu} [\hat{Q}_{\mu}^{\text{S}}, \tilde{Q}_{\mu}\rho_{\text{S}}(t) - \rho_{\text{S}}(t)\tilde{Q}_{\mu}^{\dagger}], \quad (19)$$

with

$$\tilde{Q}_{\mu} \equiv \sum_{\nu} C_{\mu\nu}(-\mathcal{L}_{\text{S}})\hat{Q}_{\nu}^{\text{S}}, \quad (20)$$

and

$$C_{\mu\nu}(\omega) \equiv \frac{1}{2} \int_{-\infty}^{\infty} d\tau e^{i\omega\tau} \tilde{C}_{\mu\nu}(\tau) = [C_{\nu\mu}(\omega)]^*. \quad (21)$$

To obtain the concrete form of Lindblad equation, we shall recast \hat{Q}_{μ}^{S} and \tilde{Q}_{μ} in the system eigenstate representation, $\{|m\rangle\}$ satisfying $H_{\text{S}}|m\rangle = \epsilon_m|m\rangle$, as

$$\hat{Q}_{\mu}^{\text{S}} = \sum_{mn} Q_{\mu;mn}^{\text{S}} |m\rangle\langle n|, \quad (22a)$$

$$\tilde{Q}_{\mu} = \sum_{\nu mn} C_{\mu\nu}(\omega_{nm}) Q_{\nu;mn}^{\text{S}} |m\rangle\langle n|, \quad (22b)$$

with

$$\omega_{mn} \equiv \epsilon_m - \epsilon_n \quad \text{and} \quad Q_{\mu;mn}^{\text{S}} \equiv \langle m|\hat{Q}_{\mu}^{\text{S}}|n\rangle. \quad (23)$$

We obtain

$$\dot{\rho}_{\text{S}}(t) = -i\mathcal{L}_{\text{S}}\rho_{\text{S}}(t) + \sum_{\mu\nu mn m' n'} [(\text{I}) - (\text{II}) - (\text{III})], \quad (24)$$

with

$$\begin{aligned} \text{(I)} &= [C_{\mu\nu}(\omega_{mn}) + C_{\mu\nu}(\omega_{n'm'})] \hat{S}_{\nu;m'n'} \rho_{\text{S}}(t) \hat{S}_{\mu;nm}^{\dagger}, \\ \text{(II)} &= C_{\mu\nu}(\omega_{n'm'}) \hat{S}_{\mu;nm}^{\dagger} \hat{S}_{\nu;m'n'} \rho_{\text{S}}(t), \\ \text{(III)} &= C_{\mu\nu}(\omega_{mn}) \rho_{\text{S}}(t) \hat{S}_{\mu;nm}^{\dagger} \hat{S}_{\nu;m'n'}. \end{aligned} \quad (25)$$

Here, $\hat{S}_{\mu;mn} \equiv Q_{\mu;mn}^{\text{S}} |m\rangle\langle n|$, satisfying

$$\hat{S}_{\mu;mn}^{\dagger} = Q_{\mu;nm}^{\text{S}} |n\rangle\langle m| = \hat{S}_{\mu;nm}. \quad (26)$$

Now applying the rotating wave approximation that only terms of $n' = m$ and $m' = n$ contribute, Eq. (24) gives rise to

$$\begin{aligned} \dot{\rho}_{\text{S}}(t) = -i\mathcal{L}_{\text{S}}\rho_{\text{S}}(t) + \sum_{\mu\nu mn} C_{\mu\nu}(\omega_{mn}) & \left[2\hat{S}_{\nu;nm} \rho_{\text{S}}(t) \hat{S}_{\mu;nm}^{\dagger} \right. \\ & \left. - \hat{S}_{\mu;nm}^{\dagger} \hat{S}_{\nu;nm} \rho_{\text{S}}(t) - \rho_{\text{S}}(t) \hat{S}_{\mu;nm}^{\dagger} \hat{S}_{\nu;nm} \right]. \end{aligned} \quad (27)$$

The detailed-balance relation reads

$$C_{\mu\nu}(\omega) = J_{\mu\nu}(\omega)[1 + \bar{n}(\omega)] = J_{\nu\mu}(-\omega)\bar{n}(-\omega). \quad (28)$$

Note that $J_{\nu\mu}(-\omega) = -J_{\mu\nu}(\omega)$ and $\bar{n}(\omega) + \bar{n}(-\omega) = -1$ where $\bar{n}(\omega) = 1/(e^{\beta\omega} - 1)$. We obtain readily

$$\dot{\rho}_s(t) = \left[-i\mathcal{L}_s + \sum_{\mu\nu mn} (L_{\mu\nu mn}^{(+)} + L_{\mu\nu mn}^{(-)}) \right] \rho_s(t) \quad (29)$$

where $[\bar{n}_{mn} \equiv \bar{n}(\omega_{mn})]$

$$L_{\mu\nu mn}^{(+)} \hat{O} = \frac{1}{2} J_{\mu\nu}(\omega_{mn}) (1 + \bar{n}_{mn}) \left(2\hat{S}_{\nu;nm} \hat{O} \hat{S}_{\mu;nm}^\dagger - \hat{S}_{\mu;nm}^\dagger \hat{S}_{\nu;nm} \hat{O} - \hat{O} \hat{S}_{\mu;nm}^\dagger \hat{S}_{\nu;nm} \right), \quad (30a)$$

$$L_{\mu\nu mn}^{(-)} \hat{O} = \frac{1}{2} J_{\nu\mu}(\omega_{mn}) \bar{n}_{mn} \left(2\hat{S}_{\nu;nm}^\dagger \hat{O} \hat{S}_{\mu;nm} \right)$$

$$- \hat{S}_{\mu;nm} \hat{S}_{\nu;nm}^\dagger \hat{O} - \hat{O} \hat{S}_{\mu;nm} \hat{S}_{\nu;nm}^\dagger \right). \quad (30b)$$

This is just the standard form of Lindblad master equation.^{24,25} It is also equivalent to the secular Redfield equation.^{38,39}

In comparison with DEOM for the non-Markovian influence of phonon bath, the Markovian Lindblad master equation treatment in Sec. III is as the above Eq. (29) with Eq. (30). Note that the system eigenstate representation shall be adopted. For the photon bath with the single coupling mode $\hat{Q}_1^{(I)}$ in Sec. II A, we finally obtain Eq. (10) with Eq. (11).

* Contributed equally to this work

† Electronic address: wy2010@ustc.edu.cn

‡ Electronic address: rxxu@ustc.edu.cn

- ¹ V. R. Policht, A. Niedringhaus, R. Willow, P. D. Laible, D. F. Bocian, C. Kirmaier, D. Holten, T. Mančal, and J. P. Ogilvie, “Hidden vibronic and excitonic structure and vibronic coherence transfer in the bacterial reaction center,” *Sci. Adv.* **8**, eabk0953 (2022).
- ² J. S. Cao, R. J. Cogdell, D. F. Coker, H.-G. Duan, J. Hauer, U. Kleinekathöfer, T. L. C. Jansen, T. Mančal, R. J. D. Miller, J. P. Ogilvie, V. I. Prokhorenko, T. Renger, H.-S. Tan, R. Tempelaar, M. Thorwart, E. Thyrhaug, S. Westenhoff, and D. Zigmantas, “Quantum biology revisited,” *Sci. Adv.* **6**, eaaz4888 (2020).
- ³ E. Romero, V. I. Novoderezhkin, and R. van Grondelle, “Quantum design of photosynthesis for bio-inspired solar-energy conversion,” *Nature* **543**, 355 (2017).
- ⁴ E. Romero, R. Augulis, V. I. Novoderezhkin, M. Ferretti, J. Thieme, D. Zigmantas, and R. van Grondelle, “Quantum coherence in photosynthesis for efficient solar-energy conversion,” *Nat. Phys.* **10**, 676 (2014).
- ⁵ F. D. Fuller, J. Pan, A. Gelzinis, V. Butkus, S. S. Senlik, D. E. Wilcox, C. F. Yocom, L. Valkunas, D. Abramavicius, and J. P. Ogilvie, “Vibronic coherence in oxygenic photosynthesis,” *Nat. Chem.* **6**, 706 (2014).
- ⁶ E. Romero, I. H. M. van Stokkum, V. I. Novoderezhkin, J. P. Dekker, and R. van Grondelle, “Two Different Charge Separation Pathways in Photosystem II,” *Biochemistry* **49**, 4300 (2010).
- ⁷ E. Collini, C. Y. Wong, K. E. Wilk, P. M. G. Curmi, P. Brumer, and G. D. Scholes, “Coherently wired light-harvesting in photosynthetic marine algae at ambient temperature,” *Nature* **463**, 644 (2010).
- ⁸ G. S. Engel, T. R. Calhoun, E. L. Read, T. K. Ahn, T. Mančal, Y. C. Cheng, R. E. Blankenship, and G. R. Fleming, “Evidence for wavelike energy transfer through quantum coherence in photosynthetic systems,” *Nature* **446**, 782 (2007).
- ⁹ H. Lee, Y.-C. Cheng, and G. R. Fleming, “Coherence dynamics in photosynthesis: Protein protection of excitonic coherence,” *Science* **316**, 1462 (2007).
- ¹⁰ A. Ishizaki and G. R. Fleming, “Unified treatment of quantum coherent and incoherent hopping dynamics in electronic energy transfer: Reduced hierarchy equation approach,” *J. Chem. Phys.* **130**, 234111 (2009).
- ¹¹ C. Kreisbeck, T. Kramer, M. Rodríguez, and B. Hein, “High-performance solution of hierarchical equations of motion for studying energy transfer in light-harvesting complexes,” *J. Chem. Theory Comput.* **7**, 2166 (2011).
- ¹² L. P. Chen, R. H. Zheng, Y. Y. Jing, and Q. Shi, “Simulation of the two-dimensional electronic spectra of the Fenna-Matthews-Olson complex using the hierarchical equations of motion method,” *J. Chem. Phys.* **134**, 194508 (2011).
- ¹³ J. Xu, H. D. Zhang, R. X. Xu, and Y. J. Yan, “Correlated driving and dissipation in two-dimensional spectroscopy,” *J. Chem. Phys.* **138**, 024106 (2013).
- ¹⁴ A. Chenu and G. D. Scholes, “Coherence in Energy Transfer and Photosynthesis,” *Annu. Rev. Phys. Chem.* **66**, 69 (2015).
- ¹⁵ H. D. Zhang, Q. Qiao, R. X. Xu, and Y. J. Yan, “Effects of Herzberg–Teller vibronic coupling on coherent excitation energy transfer,” *J. Chem. Phys.* **145**, 204109 (2016).
- ¹⁶ S. J. Jang and B. Mennucci, “Delocalized excitons in natural light-harvesting complexes,” *Rev. Mod. Phys.* **90**, 035003 (2018).
- ¹⁷ S. Kundu and N. Makri, “Real-time path integral simulation of exciton-vibration dynamics in light-harvesting bacteriochlorophyll aggregates,” *The Journal of Physical Chemistry Letters* **11**, 8783 (2020).
- ¹⁸ Y. Yan, Y. Liu, T. Xing, and Q. Shi, “Theoretical study of excitation energy transfer and nonlinear spectroscopy of photosynthetic light-harvesting complexes using the non-perturbative reduced dynamics method,” *WIREs Comp. Mol. Sci.* **11**, e1498 (2021).
- ¹⁹ S. Kundu and N. Makri, “Intramolecular Vibrations in Excitation Energy Transfer: Insights from Real-Time Path Integral Calculations,” *Annual Review of Physical Chemistry* **73** (2022).
- ²⁰ M. Wertnik, A. Chin, F. Nori, and N. Lambert, “Optimizing co-operative multi-environment dynamics in a dark-state-enhanced photosynthetic heat engine,” *J. Chem. Phys.* **149**, 084112 (2018).
- ²¹ M. Qin, H. Shen, X. Zhao, and X. Yi, “Effects of system-bath coupling on a photosynthetic heat engine: A polaron master-equation approach,” *Phys. Rev. A* **96**, 012125 (2017).
- ²² C. Creatore, M. A. Parker, S. Emmott, and A. W. Chin, “Efficient biologically inspired photocell enhanced by delocalized quantum states,” *Phys. Rev. Lett.* **111**, 253601 (2013).
- ²³ K. E. Dorfman, D. V. Voronine, S. Mukamel, and M. O. Scully, “Photosynthetic reaction center as a quantum heat engine,” *Proc. Natl. Acad. Sci.* **110**, 2746 (2013).
- ²⁴ G. Lindblad, “On the generators of quantum dynamical

semigroups,” *Commun. Math. Phys.* **48**, 119 (1976).

²⁵ V. Gorini, A. Kossakowski, and E. C. G. Sudarshan, “Completely positive dynamical semigroups of N -level systems,” *J. Math. Phys.* **17**, 821 (1976).

²⁶ Y. J. Yan, “Theory of open quantum systems with bath of electrons and phonons and spins: Many-dissipaton density matrixes approach,” *J. Chem. Phys.* **140**, 054105 (2014).

²⁷ H. D. Zhang, R. X. Xu, X. Zheng, and Y. J. Yan, “Nonperturbative spin-boson and spin-spin dynamics and nonlinear Fano interferences: A unified dissipaton theory based study,” *J. Chem. Phys.* **142**, 024112 (2015).

²⁸ Y. Tanimura, “Numerically “exact” approach to open quantum dynamics: The hierarchical equations of motion (HEOM),” *J. Chem. Phys.* **153**, 020901 (2020).

²⁹ Y. Tanimura and R. Kubo, “Time evolution of a quantum system in contact with a nearly Gaussian-Markovian noise bath,” *J. Phys. Soc. Jpn.* **58**, 101 (1989).

³⁰ Y. A. Yan, F. Yang, Y. Liu, and J. S. Shao, “Hierarchical approach based on stochastic decoupling to dissipative systems,” *Chem. Phys. Lett.* **395**, 216 (2004).

³¹ A. Ishizaki and Y. Tanimura, “Quantum dynamics of system strongly coupled to low temperature colored noise bath: Reduced hierarchy equations approach,” *J. Phys. Soc. Jpn.* **74**, 3131 (2005).

³² R. X. Xu, P. Cui, X. Q. Li, Y. Mo, and Y. J. Yan, “Exact quantum master equation via the calculus on path integrals,” *J. Chem. Phys.* **122**, 041103 (2005).

³³ R. X. Xu and Y. J. Yan, “Dynamics of quantum dissipation systems interacting with bosonic canonical bath: Hierarchical equations of motion approach,” *Phys. Rev. E* **75**, 031107 (2007).

³⁴ Z.-H. Chen, Y. Wang, R.-X. Xu, and Y. Yan, “Correlated vibration–solvent effects on the non-Condon exciton spectroscopy,” *J. Chem. Phys.* **154**, 244105 (2021).

³⁵ U. Weiss, *Quantum Dissipative Systems*, World Scientific, Singapore, 2021, 5th ed.

³⁶ Y. J. Yan and R. X. Xu, “Quantum mechanics of dissipative systems,” *Annu. Rev. Phys. Chem.* **56**, 187 (2005).

³⁷ Y. J. Yan, “Quantum Fokker-Planck theory in a non-Gaussian-Markovian medium,” *Phys. Rev. A* **58**, 2721 (1998).

³⁸ Y. J. Yan, F. Shuang, R. X. Xu, J. X. Cheng, X. Q. Li, C. Yang, and H. Y. Zhang, “Unified approach to the Bloch-Redfield theory and quantum Fokker-Planck equations,” *J. Chem. Phys.* **113**, 2068 (2000).

³⁹ A. G. Redfield, “The theory of relaxation processes,” *Adv. Magn. Reson.* **1**, 1 (1965).